HHS Public Access

Author manuscript

Curr Eye Res. Author manuscript; available in PMC 2023 January 01.

Published in final edited form as:

Curr Eye Res. 2022 January ; 47(1): 79–90. doi:10.1080/02713683.2021.1945109.

Identification of missense extracellular matrix gene variants in a large glaucoma pedigree and investigation of the N700S thrombospondin-1 variant in normal and glaucomatous trabecular meshwork cells.

Mary K. Wirtz[1], **Renee Sykes**[1], **John Samples**[2], **Beth Edmunds**[1], **Dongseok Choi**[1,3,4], **Douglas R. Keene**[5], **Sara F. Tufa**[5], **Ying Ying Sun**[1], **Kate E. Keller**[1,6,#]

[1]Casey Eye Institute, Oregon Health & Science University, Portland, OR 97239.

[2]Washington State University, Spokane, WA, 99202.

[3]OHSU-PSU School of Public Health Oregon Health & Science University, Portland, OR 97239.

[4]Graduate School of Dentistry, Kyung Hee University, Seoul, Korea

[5]Shriners Hospitals for Children, Portland, OR 97239

[6]Department of Chemical Physiology and Biochemistry, Oregon Health & Science University, Portland, OR 97239.

Abstract

Purpose: Primary open angle glaucoma (POAG) is a complex heterogeneous disease. While several POAG genes have been identified, a high proportion of estimated heritability remains unexplained. Elevated intraocular pressure (IOP) is a leading POAG risk factor and dysfunctional extracellular matrix (ECM) in the trabecular meshwork (TM) contributes to elevated IOP. In this study, we sought to identify missense variants in ECM genes that correlate with ocular hypertensive POAG.

Methods: Whole genome sequencing was used to identify genetic variants in five members of a large POAG family (n=68) with elevated IOP. The remaining family members were screened by Sanger sequencing. Unrelated normal (NTM) and glaucomatous (GTM) cells were sequenced for the identified variants. ECM protein levels were determined by Western immunoblotting and confocal and electron microscopy investigated ECM ultrastructural organization.

Results: Three ECM gene variants were significantly associated with POAG or elevated IOP in a large POAG pedigree. These included rs2228262 (N700S; thrombospondin-1 (*THBS1*, TSP1)), rs112913396 (D563G; collagen type VI, alpha 3 (*COL6A3*)) and rs34759087 (E987K; laminin subunit beta 2 (*LAMB2*)). Screening of unrelated TM cells (n=27) showed higher prevalence of the *THBS1* variant, but not the *LAMB2* variant, in GTM cells (39%) than NTM cells (11%). The rare *COL6A3* variant was not detected. TSP1 protein was upregulated and COL6A3 was down-regulated in TM cells with N700S subject to mechanical stretch, an *in vitro* method that mimics elevated IOP. Immunofluorescence showed increased TSP1 immunostaining in cell strains

[#]To whom correspondence should be addressed: 503 494 2366, gregorka@ohsu.edu.

with N700S compared to wild-type TM cells. Ultrastructural studies showed ECM disorganization and altered collagen type VI distribution in GTM versus NTM cells.

Conclusions: Our results suggest that missense variants in ECM genes may not cause catastrophic changes to the TM, but over many years, subtle changes in ECM may accumulate and cause structural disorganization of the outflow resistance leading to elevated IOP in POAG patients.

Introduction

By 2040, over 100 million individuals worldwide will have developed glaucoma, a blinding disease resulting from irreversible damage to the optic nerve[1]. Primary open angle glaucoma (POAG) is the most common form of glaucoma in Western and African nations[1]. Because of the subtlety of the disease in its early stages and limited public awareness of glaucoma and its risk factors, many individuals with this disease remain undiagnosed until severe and usually bilateral visual field loss has occurred[2].

Elevated intraocular pressure (IOP) is a leading risk factor for POAG and lowering of IOP is the only effective treatment for preserving vision in glaucoma patients to date[3]. Elevated IOP eventually damages optic nerve axons, leading to retinal ganglion cell death and ultimately to impairment of vision in glaucoma patients[3–5]. IOP is established by the relationship between the rate of production of aqueous humor and drainage from the eye, which is predominantly through the conventional outflow system comprised of the trabecular meshwork (TM) and Schlemm's canal. The TM's primary function is to regulate the outflow of the aqueous humor from the anterior chamber into Schlemm's canal. It maintains this homeostasis by building a modifiable resistance to aqueous humor outflow, which is primarily comprised of extracellular matrix (ECM)[6]. When IOP elevates in normal individuals, cells in the juxtacanalicular (JCT) region of the TM become mechanically stretched and a complex program of ECM remodeling occurs[6–10]. This modified resistance allows greater aqueous outflow, which then leads to reduction in pressure[6, 11]. If aqueous drainage is impaired, such as in glaucoma, pressure will not normalize, or may even increase further. The ECM of glaucomatous TM is distinct from normal TM[6, 11–15]. Morphologically, the elastic fiber network becomes thickened with the appearance of sheath-derived plaques of extracellular material[12, 14]. These plaques accumulate in POAG TM compared to age-matched normal tissue. Proteomics revealed differential levels of several ECM proteins in POAG TM compared to control[13] and immunoelectron microscopy localized collagen type VI to these plaques[16]. Furthermore, gene expression studies have delineated the importance of specific ECM molecules for remodeling the TM in response to elevated IOP, or mechanical stretching as a surrogate for elevated IOP[8, 11, 17, 18].Thus, ECM synthesis, composition and remodeling is critical to the regulation of IOP.

Several genes involved in POAG pathogenesis have been identified in Mendelian studies including *MYOC*, *IL20RB*, *ASB10*, *OPTN*, *WDR36*, and *TBK1*[19–24]. Additional POAG genes have been identified by genome-wide association studies (GWAS) such as *CAV1/CAV2, CDKN2BAS, TGFBR3, FNDC3B, CADM2* and *SIX6*[25, 26]. However, only a small part of the heritability of POAG, approximately 1%, is explained by these variants[27, 28].

In addition, the genes identified by GWAS have modest per-allele genetic effect sizes (OR, ~1.1 to 3) with risk alleles often present at high frequencies (>10%) in control populations[29, 30]. In contrast, high-penetrance genetic mutations, such as in *MYOC*, observed in families have diagnostic as well as predictive values[31]. In addition to these Mendelian and GWAS studies on POAG, variants in several ECM genes are linked to POAG endophenotypes. For instance, GWAS studies have identified the association of *COL6A3* and *LTBP1* with IOP[32], and *COL5A1* with central cornea thickness[33, 34].

Pedigrees have the power to detect rare genetic variants that may be missed in large association studies including GWAS. In this study, we investigated a large family comprised of 68 individuals, 20 of whom have been diagnosed with high tension POAG. We focused on identifying missense variants in ECM genes because we hypothesized these may disrupt the composition and/or organization of the outflow resistance, thus leading to glaucomatous ECM changes in the TM and elevated IOP.

Materials and Methods

Subjects

This study was approved by the Oregon Health & Science University Institutional Review Board following the principles set out in the Declaration of Helsinki. We examined and obtained blood samples from 68 members of a large Oregon family after obtaining written informed consent. Family members were examined by gonioscopy with a 4-mirror lens (Carl Zeiss Inc, Thornwood, NY) using the Becker-Schaffer grading system. A Humphrey field analyzer (Carl Zeiss Ophthalmic Systems, Dublin, CA) using the 30–2 test point pattern was used to measure visual fields. The family members, age 41 or older, were categorized into four groups: POAG, ocular hypertensives (OHT), suspects and clinically normal. POAG status was based on the following criteria: (1) treatment for glaucoma had been instigated prior to our study; or (2) two or more of the following findings were present; (a) untreated IOP of 24 mm Hg measured by Goldman applanation tonometry[35]; (b) abnormal Humphrey glaucoma hemifield test; (c) nerve fiber layer analysis and/or optic nerve head showed moderately advanced glaucomatous damage (i.e., a vertical cup/disk ratio >0.7 with or without erosion of the rim)[36]; or (3) abnormal glaucoma hemifield test. The elevated IOP group consisted of family members with an IOP ≥ 22 mmHg using Goldman applanation tonometry on two or more occasions, in whom there were no other signs of glaucoma. The suspect group consisted of family members with suspicious discs, and/or normal or borderline visual field defects and IOP measurements below 21 mmHg.

Genomic DNA isolation and next-generation sequencing

A standard salting-out procedure[20] was used to isolate genomic DNA from blood samples from all family members. Whole genome sequencing (WGS) was performed commercially on DNA samples from five family members at Macrogen (Korea). WGS covers approximately 96% of the entire human genome (3 gigabases). Exons are not only covered more effectively than using an exome sequencing approach, but variants falling outside of current exome capture designs (such as promoter or other regulatory variants) are not missed. Sequencing was performed on a HiSeq2000 (Illumina, San Diego, CA)

to an average depth of 30x for the five samples. A total of 127,373 to 135,944 Mb was identified in the five individuals with 86.65 to 90.16% of ≥ Q30 bases. The mean quality score ranged from 34.45 to 35.53. VCF files were uploaded to the Golden Helix SNP & Variation Suite and the sequences were aligned with the GRCh37/hg19 assembly. The confidence filter retained variants with a call quality of at least 20 and read depth at least 30. Bioinformatics analyses were performed following Genome Analysis Toolkit (GATK) best practices[37, 38]. Filtration for nonsynonymous sequences was followed by in-silico prediction of functionality using PolyPhen, SIFT and LRT[39–42].

Polymerase chain reaction and Sanger sequencing

Primers were designed to amplify each SNP using Primer3 through the UCSC Human Genome Browser ExonPrimer command (http://genome.ucsc.edu/cgi-bin/hgGateway) and obtained from Integrated DNA Technologies, Inc. (San Diego, CA). Polymerase chain reaction (PCR) reagents were purchased from Roche Applied Science Division (Indianapolis, IN). RED*taq* Polymerase was obtained from Sigma-Aldrich (St. Louis, MO). Standard touch-down protocols on a Gene Amp PCR System 9700 (Applied BIosystems, Inc., Foster City, CA) were used to PCR the SNPS in the genomic DNA. The PCR products were purified using ExoSAP-IT according to the manufacturer's instructions (USB Corporation, Cleveland, OH). The purified products were sequenced on an ABI 3130XL Genetic Analyzer at the Oregon Clinical and Translational Research Institute (OCTRI, Oregon Health & Science University, Portland, OR). Sequencer 4.9 (Gene Codes Corporation, Ann Arbor, MI) was used to analyze the sequencing chromatograms.

Human TM cell culture and Sanger sequencing

Normal (NTM) and glaucomatous (GTM) primary human TM cell strains were established from the dissected tissue of cadaver eyes following standard procedures[43]. Demographics of the donors are shown in Table 4. Each cell strain was previously characterized by induction of myocilin by two week's treatment with dexamethasone and used until passage 6[44, 45]. Genomic DNA was harvested from the TM cells and cleaned by treatment with ExoSAP-IT. PCR was used to amplify DNA surrounding the SNP of interest. The following primers were used: *THBS1*: 5'-CAGAGGTAACCCACACTCTTC-3' and 5'-CAAGTCATGCTTTGCTGGTATT-3'; *COL6A3*, rs112913396: 5'-TATCCAGGTGGCAGTGG-3' and 5'-GATGAACACCAGGGAGGA; *COL6A3*, rs11690358: 5'-ACTGACATTCCAGAGAG-3' and 5'-CCAAGCCTGTGACTATTAT-3'; *COL5A3*: 5'-CAGTCACTCACCGGGAT-3' and 5'-AGAGGTGAGAACTCTTGGG-3'; *LAMB2*: 5'-AGCACAGTAGTCAAGAG-3' and 5'-TATTCCCAGCAGATTGT-3'; *LAMAC2*: 5'-TCTTCTTCTTCTTTCCTTTC-3' and 5'-TGATAATCCCAACCTCTTA-3'; and *LTBP3*: 5'-GAGAAGAGCCTGTGTTT-3' and 5'-AGGTGAGAATGTGGTATC-3'. Sanger sequencing was performed at OCTRI as above.

Mechanical stretch

TM cells were subjected to static mechanical stretch, a proxy for elevated IOP[9]. Briefly, each TM cell strain was grown for 3 days on collagen type I-coated silicone membranes of 6-well BioFlex plates (Flexcell International Corp., Burlington, NC). Confluent TM cells were then washed and placed in serum-free Dulbecco's Modified Eagle's Medium

(DMEM). To produce the static stretch, the silicone membrane was centered upon the head of a pushpin and then a weight was placed on top of the lid of the tissue culture plate. This produces an upward deformation of the silicone membrane, with an estimated 10% increase in surface area[9]. For each TM cell strain, one well was mechanically stretched for 24 hours while one well was a non-stretched control. At the end of the experiment, serum-free media were harvested and proteins were separated by SDS-PAGE. Western immunoblots were performed using the following antibodies: TSP1 mouse monoclonal, clone A6.1 (cat# MA5–13398; Thermo Fisher Scientific, Waltham, MA); Laminin beta-2 rabbit polyclonal (Cat# HPA001885; MilliporeSigma, St Louis, MO); collagen type 6A3 mouse monoclonal, clone 3C4 (cat# Mab1944; MilliporeSigma); and fibronectin rabbit polyclonal (cat# Ab2413; Abcam, Cambridge, MA). After incubation with secondary antibodies (IRDye 700-conjugated anti-rabbit and IRDye 800-conjugated anti-mouse (Rockland Immunochemicals, Gilbertsville, PA)), the membranes were imaged using the Odyssey infrared imaging system (Licor Biosciences, Lincoln, NE). FIJI software was used to quantitate the intensity of each of the bands. Values for stretched samples were divided by non-stretched controls to produce a fold change. Fold changes for all NTM wild-type (n=10), TSP1 N700S variant (n=4) and GTM wild-type (n=6) cell strains were then averaged. At least three technical replicates were performed.

Confocal microscopy

To investigate ECMs produced by TM cell strains with and without the TSP1 N700S variant, we performed confocal microscopy. TM cell strains were grown for 3 days on collagen type-I coated Flexcell plates and then fixed with 4% paraformaldehyde. After blocking, the ECMs were immunostained with the TSP1 mouse monoclonal, clone A6.1 antibody or the collagen type 6A3 mouse monoclonal, clone 3C4, antibody. Secondary antibodies were Alexa Fluor 488-conjugated anti-mouse. Coverslips were mounted in ProLong gold and the slides were imaged using an Olympus FV1000 confocal microscope. Confocal acquisition settings were identical for each TM cell strain (NTM wild-type (n=10), TSP1 N700S variant (n=4) and GTM wild-type (n=6) cell strains). At least three technical replicates were performed for each cell strain. Post-acquisition, images were processed using FIJI software.

Electron Microscopy

The ECMs synthesized by TM cells in culture were processed and examined by transmission electron microscopy as described previously[46]. TM cell cultures were grown on type-I collagen coated Bioflex plates for 7 days to allow their matrices to assemble. A 4-mm punch was used to remove individual plugs from the culture surface. Some plugs were prepared for electron microscopy by immersion in 1.5% glutaraldehyde/1.5% paraformaldehyde in Dulbecco's serum free media (SFM) containing 0.05% tannic acid for a minimum of one hour followed by an extensive rinse in SFM, then post-fixation in 1% OsO4. The samples were washed in SFM then dehydrated in a graded series of ethanol to 100%, rinsed in propylene oxide and infiltrated in Spurrs epoxy over a total time of two hours, accelerated via microwave energy. Samples were polymerized at 70 °C over 18 hours. Additional plugs were prepared by extensively rinsing in SFM then immersing in collagen type 6A3 mouse monoclonal, clone 3C4 antibody diluted 1:5 in SFM overnight at 4 °C, rinsed extensively in SFM, then incubated overnight at 4 °C in goat-anti-mouse secondary antibody

conjugated to 1.4nm colloidal gold (Aurion, Wageningen, The Netherlands) diluted 1:3 in SFM. Following an extensive rinse in SFM, the samples were exposed to gold enhancement solution (Nanoprobes, Yaphank, NY) 15 minutes on ice, then rapidly warmed to 25 °C and incubated an additional 5 minutes. The samples were then rinsed with ice-cold SFM, then fixed and embedded as above. Ultrathin sections were collected onto formvar coated slot grids, stained in Uranyl acetate and lead citrate, then imaged using a FEI G2 electron microscope operated at 120KV.

Statistical Analysis

Descriptive analysis was performed by generating frequency tables for each allele by clinical conditions. The associations between an allele and clinical condition were tested by $\chi 2$-tests and the corresponding p-values were estimated by simulations. As a multiple test correction, all p-values of $\chi 2$-tests for a clinical variable were adjusted by the Holm's method[47]. For those alleles with $p < 0.1$ in $\chi 2$-tests, logistic regression models were fitted to estimate the odds ratios of clinical conditions relative to normal group. All computations were performed by R statistical language (http://www.r-project.org). The family-based association test using generalized estimating equations (FBAT-GEE) was used to examine the ECM variants across the family[48]. For densitometry data, one-way ANOVA with Tukey's post-hoc correction was performed where $p<0.05$ was considered significant. For analysis of *THBS1* variant frequency in normal and glaucomatous TM cell strains, a Fisher's exact test was performed. The "n" for each experiment is stated in the figure legends.

Results

A large pedigree with POAG and elevated IOP segregating through six generations was identified (Figure 1). For this study, only those family members over the age of 40 were included, comprising 68 family members, including 29 women and 39 men. Half of the family members had normal ocular findings (n=34), 20 were diagnosed with POAG, six were OHTs and eight were glaucoma suspects based upon optic nerve findings (Table 1). The age of diagnosis for POAG ranged from 38 to 79. Approximately half of the individuals with POAG were male (n=11). Many of the POAG family members had untreated IOPs >30 mmHg with one member having an untreated IOP of 44 mmHg. While two individuals did not have recorded IOP's over 21 mmHg, one of them had already had surgery on their left eye by the time of the study exam.

Previously, linkage analysis in this family had been suggestive of a POAG gene in a region on chromosome 5 containing the WDR36 gene with a two-point logarithm of the odds (LOD) score of 2.71[49]. Sequencing of WDR36 revealed no disease-causing mutations that segregated with POAG in this family. Since the LOD score did not reach 3 in this region or on any other chromosome, it suggests that the basis of POAG in this family is complex and most likely results from more than one gene.

To identify potential POAG-causing or -susceptibility genetic variants, WGS of five family members with POAG was performed (boxed in symbols in Figure 1). These five family members were chosen because each came from a separate sibship, which should help eliminate variants shared based on close relationship. Numerous non-synonymous SNPs

were identified, with the number of variants ranging between 214 and 271 for each individual after filtering for coding variants predicted to be deleterious was performed. Only one variant was identified, rs41276257, Rho related BTB domain containing 3 (*RHOBTB3*) that was present in all five individuals. This SNP is on chromosome 5 just outside of the POAG region mapped by linkage analysis. However, this variant did not segregate cleanly with POAG in this pedigree. This was not surprising since POAG is a heterogeneous disease with a statistically significant 'polygenic' component underlying disease risk[50]. We therefore focused our attention to ECM genes since IOP is regulated by remodeling of ECM and ECM proteins accumulate in glaucoma TM[6]. Many of the individuals in this family had POAG and/or elevated IOP, so we hypothesized that missense variants in ECM genes may play a role in pathogenesis. ECM genes were defined as those present in the matrisome gene sets (http://matrisomeproject.mit.edu/)[51]. After filtering for non-synonymous ECM variants present in three or more of the original five individuals, we identified missense SNPs in seven candidate ECM genes (Table 2): thrombospondin-1 (*THBS1*, rs2228262), laminin, beta 2 (*LAMB2*, rs3475908), latent transforming growth factor beta binding protein-3 (*LTBP3*, rs11545200), laminin subunit gamma 2 (*LAMC2*, rs11586699), collagen type V, alpha 3 (*COL5A3*, rs62638750), and two variants in collagen type VI, alpha 3 (*COL6A3*, rs*112913396 and* rs*11690358*). Based on the minor allele frequency in the 1000 genomes database[52], rs*112913396* is considered rare (0.1%), while the rs*11690358* is common (11.2%).

Sanger sequencing of these seven ECM variants was performed in all 68 family members. As shown in Table 3, the *THBS1* SNP, rs2228262, was significantly associated with POAG in this family ($p<0.031$ after correction for multiple tests with an odds ratio of 0.29 (95% confidence interval 0.12 ~ 0.44)). In addition, the rare *COL6A3* variant, *rs112913396*, but not the common *COL6A3* variant, *rs11690358*, was significantly associated with POAG ($p<0.031$) (Table 3). To correct for potential bias based on increased sharing of alleles from family relationships, we also used FBAT-Gee analysis. With this analysis the *COL6A3* SNP rs112913396 ($p=0.03$) and *LAMB2* SNP rs34759087 ($p=0.045$) were significantly associated with POAG using an additive model with IOP as an interaction variable. The *THBS1* SNP rs228262 ($p=0.027$) was significantly associated with IOP using a dominant model with age as a predictor and CCT as an interaction variable. None of the other four ECM SNP variants were significantly associated with POAG in this family.

Since the *THBS1* N700S SNP was previously associated with myocardial infarction[53], and several members of this family have hypertension and/or heart attacks, we tested whether the identified SNPs were associated with either of these disorders. The *THBS1* SNP was not associated with hypertension, but was significantly associated with heart attack in this family (Table 3) although after Holm correction this SNP was no longer significant. The rare *COL6A3* variant, rs112913396, approached a significant *p* value for association with hypertension ($p=0.057$), but not myocardial infarction. None of the other identified SNPs were significantly associated with either hypertension or myocardial infarction in this family (Table 3).

As shown in Table 2, the *THBS1* variant is relatively common, with approximately 10% minor allele frequency in the European population reported in the 1000 genomes database[52].

Therefore, we hypothesized that some of our bank of human TM cells may harbor the variant. Sanger sequencing of NTM (n=19) and GTM (n=8) cells identified seven cell strains harboring the *THBS1* variant (Table 4). Three of these were derived from glaucomatous individuals, while two were from individuals who died aged ≤ 47 years. These persons may have been too young to have developed OHT or glaucoma. The incidence of the *THBS1* variant in normal TM cell strains (2 in 19) sequenced to date was 10.5%, which is similar to the expected frequency in the 1000 genomes database[10]. However, there was a much higher frequency (37.5%; 3 in 8) in the glaucoma cell strains. A Fisher's exact test did not show significance (p=0.135), likely due to the relatively small 'n' of the GTM cell strains. The *LAMB2* variant was detected in NTM (21%) and GTM (12.5%) cells. None of the TM cell strains harbored the rare *COL6A3* variant, rs112913396.

Mechanical stretching of TM cells *in vitro* is used as a proxy for the stresses and strains exerted by elevated IOP on TM cells *in situ*[7–9, 18]. Here, we subjected confluent wild-type NTM and GTM cells, as well as NTM and GTM cell strains with the TSP1 N700S variant to static mechanical stretch for 24 hours. The protein levels of TSP1, LAMB2, COL6A3, and fibronectin in media were investigated by Western immunoblotting (Figure 2). Because the proteins had different expression levels in each of the individual cell strains, we quantitated the intensity of each band using densitometry and calculated a ratio of the stretch to non-stretch bands for individual cell strains. When the ratios were averaged, TSP1 protein levels were significantly increased (p=0.048) in TM cells harboring the N700S variant after 24 hours of static stretch compared to wild-type NTM or GTM cells. Conversely, the levels of COL6A3 were reduced, but this did not reach significance following Tukey's post-hoc correction (Figure 2A). LAMB2, which was paired with TSP1 on the immunoblot, and fibronectin, which was paired with COL6A3, showed no significant differences in protein levels following 24 hours of stretch (Figure 2C, D). Thus, TM cells with the N700S variant upregulate their TSP1 protein levels, but decrease the amount of soluble collagen type VI, in response to mechanical stretch.

Next, we analyzed the distribution of TSP1 by immunofluorescence in TM cells subject to mechanical stretch for 24 hours. In three wild-type NTM cell strains, TSP1 assembled into fine fibrils as well as plaque-like structures (Figure 3A–C). Following 24 hours of static stretch, there were increased patches of immunostaining (Figure 3G–I). In two non-stretched TM cell strains with the N700S variant and a wild-type GTM, there was lower deposition of TSP1 than in wild-type NTM cells (Figure 3D–F). Both cell strains with the N700S variant showed increased immunostaining in the plaque-like structures after 24 hours of static stretch (Figure 3J, K), compared to their non-stretched controls. Fine fibrillar material was diminished in stretch and non-stretched N700S cells compared to three wild-type NTM cell strains.

Collagen type VI binds to TSP1[54] and so the distribution of collagen VI in NTM and GTM cells with and without the N700S variant was investigated by confocal microscopy (Figure 3M–R). Collagen type VI was expressed in wild-type normal (Figure 3M, N) and N700S NTM cells (Figure 3O, P) in approximately the same amounts and in similar distribution patterns. However, in both wild-type GTM cells (Figure 3R) and in a GTM cell strain with the N700S variant (Figure 3Q), there was a large reduction in collagen type VI

immunostaining. Images are representative of n=6 GTM cell strains. These results suggest that the amount of collagen type VI deposited into the ECM was reduced in glaucomatous TM cells, but collagen type VI deposition was not correlated with the presence of N700S.

The ultrastructure of the ECMs produced by NTM and GTM cells in culture was also investigated and immunoelectron microscopy using the COL6A3 monoclonal antibody was performed (Figure 4). Typical 100-nm periodic immunolabeling of parallel type VI microfilaments was found in NTM cells (Figure 4A, B), whereas there was much less overall COL6A3 alignment and immunolabeling in GTM cells (Figure 4C, D). COL6A3-containing microfibrils appeared to be more randomly deposited and poorly aligned compared to NTM cells. Furthermore, the characteristic 100-nm periodic immunolabeling of COL6A3 in NTM cells was not apparent in GTM cells. Thus, ECM ultrastructure differed between cultured NTM and GTM cells.

Discussion

In this study, we identified three missense variants in ECM genes, one in *THBS1*, rs2228262 (N700S), *COL6A3*, rs112913396 (D563G), and *LAMB2*, rs34759087 (E987K) which were associated with POAG or IOP in a large Oregon family. This pedigree contains 20 individuals diagnosed with high tension POAG. An initial WGS in five family members with POAG failed to identify a specific variant that segregated with glaucoma. Recognizing the complexity of this family and that glaucoma has a highly polygenic component underlying disease risk[50, 55], we focused on identifying ECM susceptibility genes based on the role of the ECM in IOP homeostasis[6, 11, 56]. Of the seven ECM genes that were identified by WGS, three genes had previously been associated with POAG endophenotypes: *LTBP3* was identified as a candidate for optic disc parameters by GWAS[57]; *COL5* was associated with central corneal thickness, a glaucoma risk factor[33, 34]; and *COL6A3* was identified in a GWAS study for elevated IOP[32]. However, only three of the seven genes identified by WGS showed association with POAG or IOP, the *THBS1* variant, rs2228262, the *COL6A3* variant, rs112913396 and the *LAMB2* variant, rs3475908. Our data suggests that the *THBS1*, *COL6A3* and *LAMB2* variants represent susceptibility genes that, in combination with other genetic and/or environmental factors, may tip the individual towards disease.

The N700S variant in TSP1 has previously been correlated with myocardial infarction in individuals, who are homozygous for the variant in American and Italian cohorts[53, 58]. However, this finding was not replicated in other populations, several of whom had no occurrence of the GG genotype in the myocardial infarction patients[59–62]. In our study, the N700S variant appeared to be associated with myocardial infarction, but after Holm correction, the p-value was no longer statistically significant. It is possible that as the family members age, a future analysis may be required to reexamine this data.

TSP1 is a matricellular protein involved in cell-cell and cell-ECM interactions[63, 64]. While TSP1 immunostains the JCT region of the inner wall of Schlemm's canal in normal human eyes, glaucoma eyes show intense TSP1 immunoreactivity[65]. Scleral tissue lining the outer wall of Schlemm's canal and surrounding collector channels have increased TSP1 immunostaining, while upregulated expression of TSP1 was also found in lamina cribrosa

cells at the optic nerve in glaucomatous eyes[64, 66]. Thus, the two major sites involved in glaucoma, the TM and the optic nerve, had higher levels of TSP1 in glaucomatous eyes than age-matched controls. Previously, TSP1-deficient mice displayed significantly lower IOP compared to wild-type mice[67]. This is contradictory to our family where IOP is elevated. However, the majority of the N700S patients are heterozygous for the variant and thus 50% of the TSP1 protein they synthesize is normal. Thus, the functional consequences of a mouse knockout, where there is no TSP1 protein, and introduction of a missense amino acid change are quite different.

TSP1 is centrally placed to play an important role in the assembly and/or organization of the ECM components of the outflow resistance. TSP1 has over 83 identified ligands including collagen type VI, numerous integrin subunits, fibronectin, SPARC, versican, fibrillin-2, proteases (MMP-2, MMP-9, transglutaminase) and growth factors (VEGFA, Secreted frizzled-related protein-1 (sFRP1), PDGF, FGF2)[54]. Several of these TSP1 interactors are linked to glaucoma or are involved in IOP regulation[11]. For instance, IOP is lower in SPARC-null mice[68], while versican is enriched in low segmental outflow TM regions[69]. Thus, in normal TM, TSP1 is ideally placed to respond to mechanical stimuli and reorganize binding of ECM ligands to maintain aqueous outflow.

The TSP1 N700S variant is located in one of the calcium-wire domains. Previous recombinant protein studies have shown that introduction of a Ser residue at this site disrupts calcium binding[70]. Another study showed that N700S destabilized adjacent protein modules, which rendered the TSP1 protein more susceptible to proteolytic digestion[71]. Thus, introduction of a missense SNP could impact several processes that lead to dysfunction in the outflow pathway. We hypothesize that the N700S does not cause catastrophic changes to the ECM. Rather, subtle changes, such as slight changes in ECM synthesis rates, accumulate over time leading to alterations in the assembly of the outflow resistance components, which ultimately leads to elevated IOP.

Our study also implicated a rare *COL6A3* variant, rs112913396, as a POAG-associated gene in this family. This missense SNP is different to the one identified in a recent IOP GWAS study, rs7599762, which is located in an intron[32]. The D563G change is in the 3rd vWFA domain of the α3(VI) chain. Collagen type VI interacts with several other ECM proteins associated with basement membranes[72]. Furthermore, collagen type VI accumulates in plaque material underlying the inner wall of Schlemm's canal in glaucomatous TM[16]. Here, our immunofluorescence and electron microscopy data show there is a major reduction in COL6A3 deposition by GTM cells compared to NTM cells. Because the alpha 3 chain is required for assembly of the full heterotrimeric collagen type VI molecule[73], this suggests that GTM cells may have an overall reduction of collagen type VI. Ultrastructurally, there was a reduction in COL6A3-containing microfibrils in GTM cells, the periodic COL6A3 immunolabeling was disrupted and the microfibrils appeared disorganized compared to NTM cells. Because other ECM proteins such as decorin and biglycan bind to collagen type VI[74], the observed ultrastructural changes likely have profound effects on the overall organization of ECM components in the TM.

The main limitation of this study design is the relatively small sample size with analysis of only one POAG family and a relatively small number of NTM and GTM cell strains. The findings of an association of the N700S *THBS1*, the D563G *COL6A3* and the E987K *LAMB2* variants may be due to "winner's curse", with larger effect sizes in the discovery isolate cohort[75]. However, the molecular biology findings of the effect of the *THBS1* variant in TM cell culture supports that the N700S may have a subtle, but significant effect upon ECM synthesis and TM morphology. POAG, similar to other complex diseases, is likely to have a polygenic architecture with the potential for thousands of common SNPs contributing to the heritability of the disease[75]. While most studies have turned to massive GWAS studies with huge populations to identify and confirm new SNPs attributing to the risk of a common disease, we have taken a different approach and used a large POAG family to ascertain potential susceptibility SNPs. Due to the complexity of the family, it is possible that there are additional SNPs awaiting discovery.

In summary, we identified three missense changes, a N700S in TSP1, a D563G in COL6A3 and a E987K in LAMB2, which were associated with POAG in a large Oregon pedigree. Functional characterization of unrelated TM cell strains harboring the TSP1 variant suggests that there is a significant alteration in the synthesis and organization of ECM components. We suggest that these missense ECM variants do not cause catastrophic changes to the TM. Instead, subtle changes to the structure and organization of the ECM outflow resistance may accumulate over many years, eventually leading to elevated IOP in POAG patients.

Acknowledgements

The authors would like to thank LionsVisionGift, Portland, OR for the procurement of normal and glaucomatous cadaver eyes used for the study. This study was supported by NIH/NEI grants EY11650 (MKW), EY019643 (KEK), EY010572 (P30 Core facility grant) and an unrestricted grant to the Casey Eye Institute from Research to Prevent Blindness, New York, NY.

REFERENCES

1. Tham YC, Li X, Wong TY, Quigley HA, Aung T, Cheng CY. Global prevalence of glaucoma and projections of glaucoma burden through 2040: A systematic review and meta-analysis. Ophthalmology 2014:121(11): 2081–2090. [PubMed: 24974815]
2. Shweikh Y, Ko F, Chan MP, Patel PJ, Muthy Z, Khaw PT, Yip J, Strouthidis N, Foster PJ, Eye UKB et al. Measures of socioeconomic status and self-reported glaucoma in the u.K. Biobank cohort. Eye (Lond) 2015:29(10): 1360–1367. [PubMed: 26315700]
3. Quigley HA. Glaucoma. Lancet 2011:377(9774): 1367–1377. [PubMed: 21453963]
4. Kwon YH, Fingert JH, Kuehn MH, Alward WL. Primary open-angle glaucoma. N Engl J Med 2009:360(11): 1113–1124. [PubMed: 19279343]
5. Tian K, Shibata-Germanos S, Pahlitzsch M, Cordeiro MF. Current perspective of neuroprotection and glaucoma. Clin Ophthalmol 2015:9(2109–2118. [PubMed: 26635467]
6. Acott TS, Vranka JA, Keller KE, Raghunathan V, Kelley MJ. Normal and glaucomatous outflow regulation. Prog Retin Eye Res 2020: 100897. [PubMed: 32795516]
7. Keller KE, Kelley MJ, Acott TS. Extracellular matrix gene alternative splicing by trabecular meshwork cells in response to mechanical stretching. Invest Ophthalmol Vis Sci 2007:48(3): 1164–1172. [PubMed: 17325160]
8. Vittal V, Rose A, Gregory KE, Kelley MJ, Acott TS. Changes in gene expression by trabecular meshwork cells in response to mechanical stretching. Invest Ophthalmol Vis Sci 2005:46(8): 2857–2868. [PubMed: 16043860]

9. Bradley JM, Kelley MJ, Zhu X, Anderssohn AM, Alexander JP, Acott TS. Effects of mechanical stretching on trabecular matrix metalloproteinases. Invest Ophthalmol Vis Sci 2001:42(7): 1505–1513. [PubMed: 11381054]
10. Mitton KP, Tumminia SJ, Arora J, Zelenka P, Epstein DL, Russell P. Transient loss of alphab-crystallin: An early cellular response to mechanical stretch. Biochem Biophys Res Commun 1997:235(1): 69–73. [PubMed: 9196037]
11. Vranka JA, Kelley MJ, Acott TS, Keller KE. Extracellular matrix in the trabecular meshwork: Intraocular pressure regulation and dysregulation in glaucoma. Exp Eye Res 2015:133(112–125. [PubMed: 25819459]
12. Rohen JW, Lutjen-Drecoll E, Flugel C, Meyer M, Grierson I. Ultrastructure of the trabecular meshwork in untreated cases of primary open-angle glaucoma (poag). Exp Eye Res 1993:56(6): 683–692. [PubMed: 8595810]
13. Bhattacharya SK, Rockwood EJ, Smith SD, Bonilha VL, Crabb JS, Kuchtey RW, Robertson NG, Peachey NS, Morton CC, Crabb JW. Proteomics reveal cochlin deposits associated with glaucomatous trabecular meshwork. J Biol Chem 2005:280(7): 6080–6084. [PubMed: 15579465]
14. Tektas OY, Lutjen-Drecoll E. Structural changes of the trabecular meshwork in different kinds of glaucoma. Exp Eye Res 2009:88(4): 769–775. [PubMed: 19114037]
15. Ueda J, Wentz-Hunter K, Yue BY. Distribution of myocilin and extracellular matrix components in the juxtacanalicular tissue of human eyes. Invest Ophthalmol Vis Sci 2002:43(4): 1068–1076. [PubMed: 11923248]
16. Lutjen-Drecoll E, Rittig M, Rauterberg J, Jander R, Mollenhauer J. Immunomicroscopical study of type vi collagen in the trabecular meshwork of normal and glaucomatous eyes. Exp Eye Res 1989:48(1): 139–147. [PubMed: 2920781]
17. Vittitow J, Borras T. Genes expressed in the human trabecular meshwork during pressure-induced homeostatic response. J Cell Physiol 2004:201(1): 126–137. [PubMed: 15281095]
18. Luna C, Li G, Liton PB, Epstein DL, Gonzalez P. Alterations in gene expression induced by cyclic mechanical stress in trabecular meshwork cells. Mol Vis 2009:15(534–544. [PubMed: 19279691]
19. Stone EM, Fingert JH, Alward WL, Nguyen TD, Polansky JR, Sunden SL, Nishimura D, Clark AF, Nystuen A, Nichols BE et al. Identification of a gene that causes primary open angle glaucoma. Science 1997:275(5300): 668–670. [PubMed: 9005853]
20. Pasutto F, Keller KE, Weisschuh N, Sticht H, Samples JR, Yang YF, Zenkel M, Schlotzer-Schrehardt U, Mardin CY, Frezzotti P et al. Variants in asb10 are associated with open-angle glaucoma. Hum Mol Genet 2012:21(6): 1336–1349. [PubMed: 22156576]
21. Rezaie T, Child A, Hitchings R, Brice G, Miller L, Coca-Prados M, Heon E, Krupin T, Ritch R, Kreutzer D et al. Adult-onset primary open-angle glaucoma caused by mutations in optineurin. Science 2002:295(5557): 1077–1079. [PubMed: 11834836]
22. Monemi S, Spaeth G, DaSilva A, Popinchalk S, Ilitchev E, Liebmann J, Ritch R, Heon E, Crick RP, Child A et al. Identification of a novel adult-onset primary open-angle glaucoma (poag) gene on 5q22.1. Hum Mol Genet 2005:14(6): 725–733. [PubMed: 15677485]
23. Fingert JH, Robin AL, Stone JL, Roos BR, Davis LK, Scheetz TE, Bennett SR, Wassink TH, Kwon YH, Alward WL et al. Copy number variations on chromosome 12q14 in patients with normal tension glaucoma. Hum Mol Genet 2011:20(12): 2482–2494. [PubMed: 21447600]
24. Keller KE, Yang YF, Sun YY, Sykes R, Gaudette ND, Samples JR, Acott TS, Wirtz MK. Interleukin-20 receptor expression in the trabecular meshwork and its implication in glaucoma. J Ocul Pharmacol Ther. 2014:30(2–3): 267–276. [PubMed: 24455976]
25. Choquet H, Wiggs JL, Khawaja AP. Clinical implications of recent advances in primary open-angle glaucoma genetics. Eye (Lond) 2020:34(1): 29–39. [PubMed: 31645673]
26. Youngblood H, Hauser MA, Liu Y. Update on the genetics of primary open-angle glaucoma. Exp Eye Res 2019:188(107795. [PubMed: 31525344]
27. Springelkamp H, Iglesias AI, Cuellar-Partida G, Amin N, Burdon KP, van Leeuwen EM, Gharahkhani P, Mishra A, van der Lee SJ, Hewitt AW et al. Arhgef12 influences the risk of glaucoma by increasing intraocular pressure. Hum Mol Genet 2015:24(9): 2689–2699. [PubMed: 25637523]

28. Hysi PG, Cheng CY, Springelkamp H, Macgregor S, Bailey JN, Wojciechowski R, Vitart V, Nag A, Hewitt AW, Hohn R et al. Genome-wide analysis of multi-ancestry cohorts identifies new loci influencing intraocular pressure and susceptibility to glaucoma. Nat Genet 2014:46(10): 1126–1130. [PubMed: 25173106]
29. Aung T, Khor CC. Glaucoma genetics: Recent advances and future directions. Asia Pac J Ophthalmol (Phila) 2016:5(4): 256–259. [PubMed: 27488067]
30. Verma SS, Cooke Bailey JN, Lucas A, Bradford Y, Linneman JG, Hauser MA, Pasquale LR, Peissig PL, Brilliant MH, McCarty CA et al. Epistatic gene-based interaction analyses for glaucoma in emerge and neighbor consortium. PLoS Genet 2016:12(9): e1006186. [PubMed: 27623284]
31. Hewitt AW, Mackey DA, Craig JE. Myocilin allele-specific glaucoma phenotype database. Hum Mutat 2008:29(2): 207–211. [PubMed: 17966125]
32. Choquet H, Thai KK, Yin J, Hoffmann TJ, Kvale MN, Banda Y, Schaefer C, Risch N, Nair KS, Melles R et al. A large multi-ethnic genome-wide association study identifies novel genetic loci for intraocular pressure. Nat Commun 2017:8(1): 2108. [PubMed: 29235454]
33. Vitart V, Bencic G, Hayward C, Skunca Herman J, Huffman J, Campbell S, Bucan K, Navarro P, Gunjaca G, Marin J et al. New loci associated with central cornea thickness include col5a1, akap13 and avgr8. Hum Mol Genet 2010:19(21): 4304–4311. [PubMed: 20719862]
34. Vithana EN, Aung T, Khor CC, Cornes BK, Tay WT, Sim X, Lavanya R, Wu R, Zheng Y, Hibberd ML et al. Collagen-related genes influence the glaucoma risk factor, central corneal thickness. Hum Mol Genet 2011:20(4): 649–658. [PubMed: 21098505]
35. Pohjanpelto PE, Palva J. Ocular hypertension and glaucomatous optic nerve damage. Acta Ophthalmol (Copenh) 1974:52(2): 194–200. [PubMed: 4406856]
36. Hitchings RA, Wheeler CA. The optic disc in glaucoma. Iv: Optic disc evaluation in the ocular hypertensive patient. Br J Ophthalmol 1980:64(4): 232–239. [PubMed: 7387958]
37. McKenna A, Hanna M, Banks E, Sivachenko A, Cibulskis K, Kernytsky A, Garimella K, Altshuler D, Gabriel S, Daly M et al. The genome analysis toolkit: A mapreduce framework for analyzing next-generation DNA sequencing data. Genome Res 2010:20(9): 1297–1303. [PubMed: 20644199]
38. Van der Auwera GA, Carneiro MO, Hartl C, Poplin R, Del Angel G, Levy-Moonshine A, Jordan T, Shakir K, Roazen D, Thibault J et al. From fastq data to high confidence variant calls: The genome analysis toolkit best practices pipeline. Curr Protoc Bioinformatics 2013:43(11 10 11–33.
39. Ramensky V, Bork P, Sunyaev S. Human non-synonymous snps: Server and survey. Nucleic Acids Res 2002:30(17): 3894–3900. [PubMed: 12202775]
40. Chun S, Fay JC. Identification of deleterious mutations within three human genomes. Genome Res 2009:19(9): 1553–1561. [PubMed: 19602639]
41. Ng PC, Henikoff S. Sift: Predicting amino acid changes that affect protein function. Nucleic Acids Res 2003:31(13): 3812–3814. [PubMed: 12824425]
42. San Lucas FA, Wang G, Scheet P, Peng B. Integrated annotation and analysis of genetic variants from next-generation sequencing studies with variant tools. Bioinformatics 2012:28(3): 421–422. [PubMed: 22138362]
43. Keller KE, Bhattacharya SK, Borras T, Brunner TM, Chansangpetch S, Clark AF, Dismuke WM, Du Y, Elliott MH, Ethier CR et al. Consensus recommendations for trabecular meshwork cell isolation, characterization and culture. Exp Eye Res 2018:171(164–173. [PubMed: 29526795]
44. Sun YY, Yang YF, Keller KE. Myosin-x silencing in the trabecular meshwork suggests a role for tunneling nanotubes in outflow regulation. Invest Ophthalmol Vis Sci 2019:60(2): 843–851. [PubMed: 30807639]
45. Sun YY, Bradley JM, Keller KE. Phenotypic and functional alterations in tunneling nanotubes formed by glaucomatous trabecular meshwork cells. Invest Ophthalmol Vis Sci 2019:60(14): 4583–4595. [PubMed: 31675075]
46. Keene DR, Tufa SF. Ultrastructural analysis of the extracellular matrix. Methods Cell Biol 2018:143(1–39. [PubMed: 29310772]
47. Holm S A simple sequentially rejective multiple test procedure. Scandinavian Journal of Statistics 1979:6(2): 65–70.

48. Lange C, Silverman EK, Xu X, Weiss ST, Laird NM. A multivariate family-based association test using generalized estimating equations: Fbat-gee. Biostatistics 2003:4(2): 195–206. [PubMed: 12925516]
49. Kramer PL, Samples JR, Monemi S, Sykes R, Sarfarazi M, Wirtz MK. The role of the wdr36 gene on chromosome 5q22.1 in a large family with primary open-angle glaucoma mapped to this region. Arch Ophthalmol 2006:124(9): 1328–1331. [PubMed: 16966629]
50. Cuellar-Partida G, Craig JE, Burdon KP, Wang JJ, Vote BJ, Souzeau E, McAllister IL, Isaacs T, Lake S, Mackey DA et al. Assessment of polygenic effects links primary open-angle glaucoma and age-related macular degeneration. Sci Rep 2016:6(26885. [PubMed: 27241461]
51. Naba A, Clauser KR, Ding H, Whittaker CA, Carr SA, Hynes RO. The extracellular matrix: Tools and insights for the “omics” era. Matrix Biol 2016:49(10–24. [PubMed: 26163349]
52. Genomes Project C, Auton A, Brooks LD, Durbin RM, Garrison EP, Kang HM, Korbel JO, Marchini JL, McCarthy S, McVean GA et al. A global reference for human genetic variation. Nature 2015:526(7571): 68–74. [PubMed: 26432245]
53. Zwicker JI, Peyvandi F, Palla R, Lombardi R, Canciani MT, Cairo A, Ardissino D, Bernardinelli L, Bauer KA, Lawler J et al. The thrombospondin-1 n700s polymorphism is associated with early myocardial infarction without altering von willebrand factor multimer size. Blood 2006:108(4): 1280–1283. [PubMed: 16684956]
54. Resovi A, Pinessi D, Chiorino G, Taraboletti G. Current understanding of the thrombospondin-1 interactome. Matrix Biol 2014:37(83–91. [PubMed: 24476925]
55. Springelkamp H, Iglesias AI, Mishra A, Hohn R, Wojciechowski R, Khawaja AP, Nag A, Wang YX, Wang JJ, Cuellar-Partida G et al. New insights into the genetics of primary open-angle glaucoma based on meta-analyses of intraocular pressure and optic disc characteristics. Hum Mol Genet 2017:26(2): 438–453. [PubMed: 28073927]
56. Keller KE, Aga M, Bradley JM, Kelley MJ, Acott TS. Extracellular matrix turnover and outflow resistance. Exp Eye Res 2009:88(4): 676–682. [PubMed: 19087875]
57. Ramdas WD, van Koolwijk LM, Ikram MK, Jansonius NM, de Jong PT, Bergen AA, Isaacs A, Amin N, Aulchenko YS, Wolfs RC et al. A genome-wide association study of optic disc parameters. PLoS Genet 2010:6(6): e1000978. [PubMed: 20548946]
58. Topol EJ, McCarthy J, Gabriel S, Moliterno DJ, Rogers WJ, Newby LK, Freedman M, Metivier J, Cannata R, O’Donnell CJ et al. Single nucleotide polymorphisms in multiple novel thrombospondin genes may be associated with familial premature myocardial infarction. Circulation 2001:104(22): 2641–2644. [PubMed: 11723011]
59. Ashokkumar M, Anbarasan C, Saibabu R, Kuram S, Raman SC, Cherian KM. An association study of thrombospondin 1 and 2 snps with coronary artery disease and myocardial infarction among south indians. Thromb Res 2011:128(4): e49–53. [PubMed: 21762961]
60. Zhou X, Huang J, Chen J, Zhao J, Ge D, Yang W, Gu D. Genetic association analysis of myocardial infarction with thrombospondin-1 n700s variant in a chinese population. Thromb Res 2004:113(3–4): 181–186. [PubMed: 15140581]
61. Abdelmonem NA, Turky NO, Hashad IM, Abdel Rahman MF, El-Etriby A, Gad MZ. Association of thrombospondin-1 (n700s) and thrombospondin-4 (a387p) gene polymorphisms with the incidence of acute myocardial infarction in egyptians. Curr Pharm Biotechnol 2017:18(13): 1078–1087. [PubMed: 29336258]
62. Boekholdt SM, Trip MD, Peters RJ, Engelen M, Boer JM, Feskens EJ, Zwinderman AH, Kastelein JJ, Reitsma PH. Thrombospondin-2 polymorphism is associated with a reduced risk of premature myocardial infarction. Arterioscler Thromb Vasc Biol 2002:22(12): e24–27. [PubMed: 12482844]
63. Adams JC, Lawler J. The thrombospondins. Cold Spring Harb Perspect Biol 2011:3(10): a009712. [PubMed: 21875984]
64. Hiscott P, Paraoan L, Choudhary A, Ordonez JL, Al-Khaier A, Armstrong DJ. Thrombospondin 1, thrombospondin 2 and the eye. Prog Retin Eye Res 2006:25(1): 1–18. [PubMed: 15996506]
65. Flugel-Koch C, Ohlmann A, Fuchshofer R, Welge-Lussen U, Tamm ER. Thrombospondin-1 in the trabecular meshwork: Localization in normal and glaucomatous eyes, and induction by tgf-beta1 and dexamethasone in vitro. Exp Eye Res 2004:79(5): 649–663. [PubMed: 15500824]

66. Kirwan RP, Wordinger RJ, Clark AF, O'Brien CJ. Differential global and extra-cellular matrix focused gene expression patterns between normal and glaucomatous human lamina cribrosa cells. Mol Vis 2009:15(76–88. [PubMed: 19145252]

67. Haddadin RI, Oh DJ, Kang MH, Villarreal G Jr., Kang JH, Jin R, Gong H, Rhee DJ. Thrombospondin-1 (tsp1)-null and tsp2-null mice exhibit lower intraocular pressures. Invest Ophthalmol Vis Sci 2012:53(10): 6708–6717. [PubMed: 22930728]

68. Haddadin RI, Oh DJ, Kang MH, Filippopoulos T, Gupta M, Hart L, Sage EH, Rhee DJ. Sparc-null mice exhibit lower intraocular pressures. Invest Ophthalmol Vis Sci 2009:50(8): 3771–3777. [PubMed: 19168904]

69. Keller KE, Bradley JM, Vranka JA, Acott TS. Segmental versican expression in the trabecular meshwork and involvement in outflow facility. Invest Ophthalmol Vis Sci 2011:52(8): 5049–5057. [PubMed: 21596823]

70. Hannah BL, Misenheimer TM, Annis DS, Mosher DF. A polymorphism in thrombospondin-1 associated with familial premature coronary heart disease causes a local change in conformation of the ca2+-binding repeats. J Biol Chem 2003:278(11): 8929–8934. [PubMed: 12643280]

71. Carlson CB, Liu Y, Keck JL, Mosher DF. Influences of the n700s thrombospondin-1 polymorphism on protein structure and stability. J Biol Chem 2008:283(29): 20069–20076. [PubMed: 18499674]

72. Cescon M, Gattazzo F, Chen P, Bonaldo P. Collagen vi at a glance. J Cell Sci 2015:128(19): 3525–3531. [PubMed: 26377767]

73. Lamande SR, Sigalas E, Pan TC, Chu ML, Dziadek M, Timpl R, Bateman JF. The role of the alpha3(vi) chain in collagen vi assembly. Expression of an alpha3(vi) chain lacking n-terminal modules n10-n7 restores collagen vi assembly, secretion, and matrix deposition in an alpha3(vi)-deficient cell line. J Biol Chem 1998:273(13): 7423–7430. [PubMed: 9516440]

74. Koudouna E, Young RD, Ueno M, Kinoshita S, Quantock AJ, Knupp C. Three-dimensional architecture of collagen type vi in the human trabecular meshwork. Mol Vis 2014:20(638–648. [PubMed: 24868138]

75. Shi J, Park JH, Duan J, Berndt ST, Moy W, Yu K, Song L, Wheeler W, Hua X, Silverman D et al. Winner's curse correction and variable thresholding improve performance of polygenic risk modeling based on genome-wide association study summary-level data. PLoS Genet 2016:12(12): e1006493. [PubMed: 28036406]

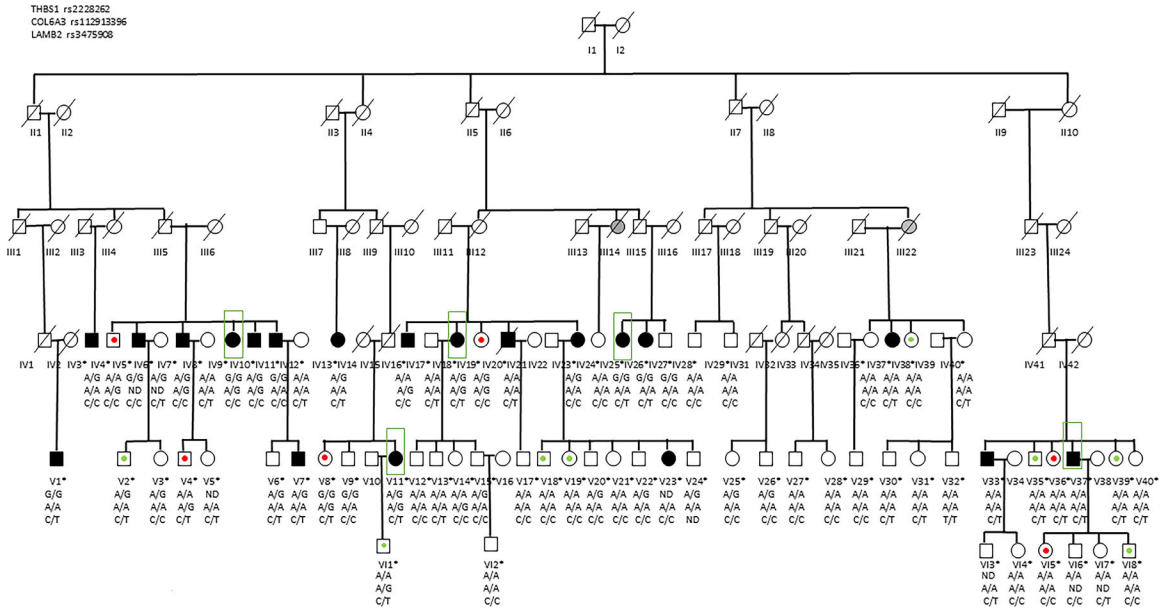

Figure 1. Pedigree of POAG family.

Blackened symbols represent individuals diagnosed with POAG. A red dot in the center of the symbol indicates elevated intraocular pressure. A green dot in the center of the symbol shows that the individual has suspicious disc or optic nerve findings. Asterisks after the ID number indicate that DNA and clinical information have been obtained for that person. The symbols filled with grey represent deceased individuals reported by the family to have had glaucoma. The SNPs are listed in the top left corner. The genotypes are listed below each person's identification number. ND = not done.

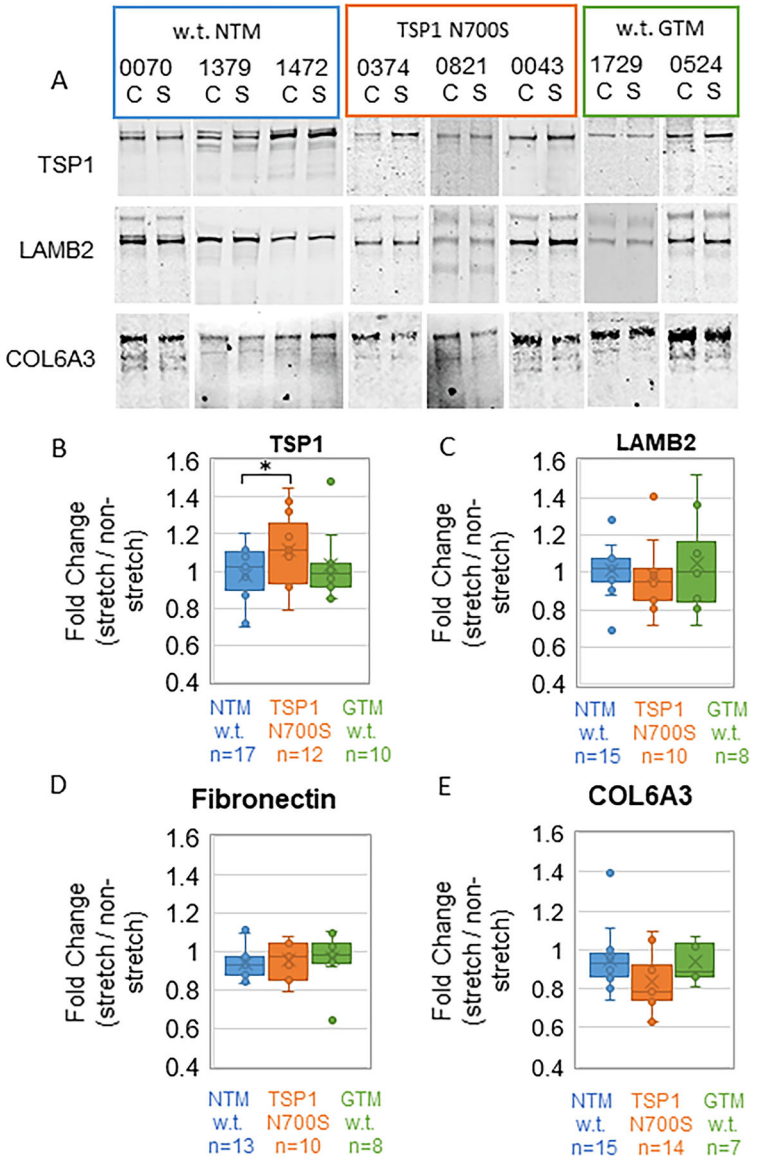

Figure 2. Quantitation of Western immunoblots of human TM cell strains.

(A) Representative Western immunoblots of TSP1 and LAMB2, which were detected on different channels (680nm and 800nm) of the same immunoblot. COL6A3 immunoblots are also shown, which were paired with fibronectin. The genotype (N700S versus wild-type (w.t.)), disease state (NTM versus GTM) and control (C) or 24 hours static mechanical stretch (S) are indicated above the blots. Densitometry was used to quantitate bands, a stretch/non-stretch ratio was calculated and the data were averaged according to TSP1 genotype of each cell strain. Box and whisker graphs show the results for TSP1 (B), LAMB2 (C), Fibronectin (D), and COL6A3 (E). Outliers are shown. The number of replicates is shown beneath each column, which includes technical replicates from n=10 wild-type NTM, n=4 N700S, and n=6 wild-type GTM cell strains. * $p<0.05$ by one-way ANOVA with Tukey's post-hoc test.

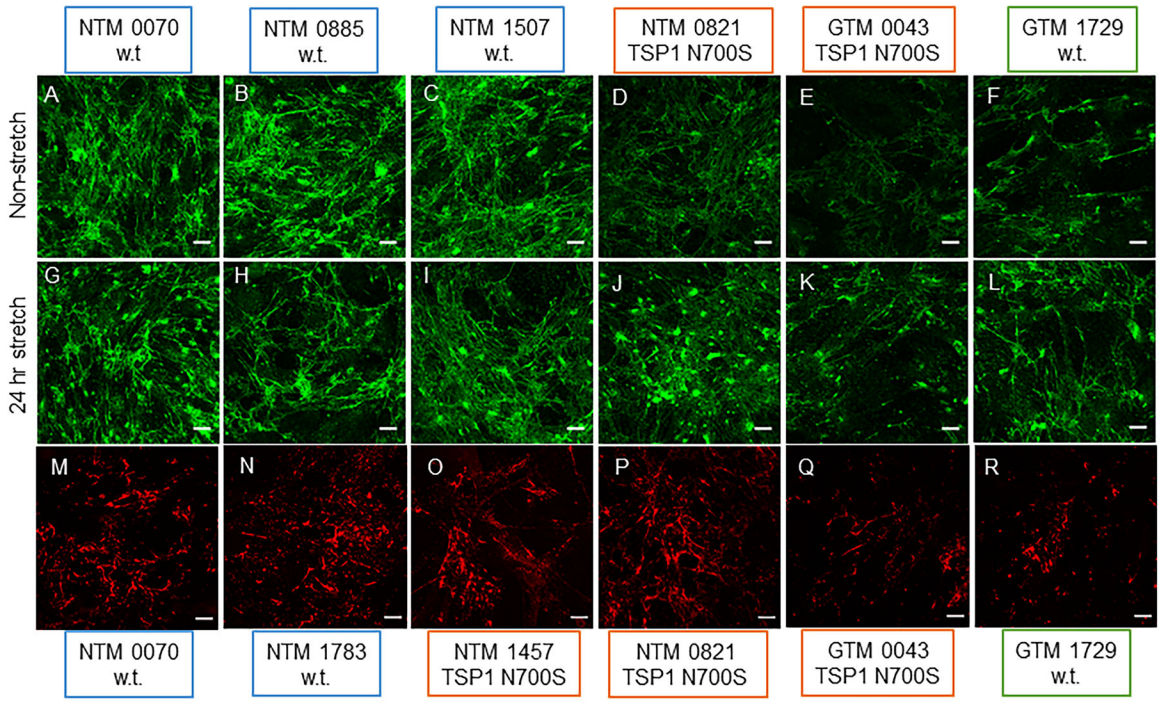

Figure 3. Immunofluorescence of TSP1 and COL6A3 in human TM cell strains with and without mechanical stretch.

Representative confocal images of wild-type NTM (A-C, G-I, M, N), wild-type GTM (F, L, R) and TM cell strains harboring the N700S variant (D, E, J, K, O-Q). TSP1 immunostaining (green) in non-stretched TM cell strains (A-F) and following 24 hours of static mechanical stretch (G-L). Representative COL6A3 distribution (red) in wild-type NTM (M. N), wild-type GTM (R), and in cell strains harboring the N700S variant (NTM (O, P) or GTM (Q)). Acquisition settings were identical for all the cell strains for each antibody. Data are representative of two technical replicates of NTM wild-type (n=3), TSP1 N700S variant (n=3) and GTM wild-type (n=3) cell strains. Scale bars = 20 μm.

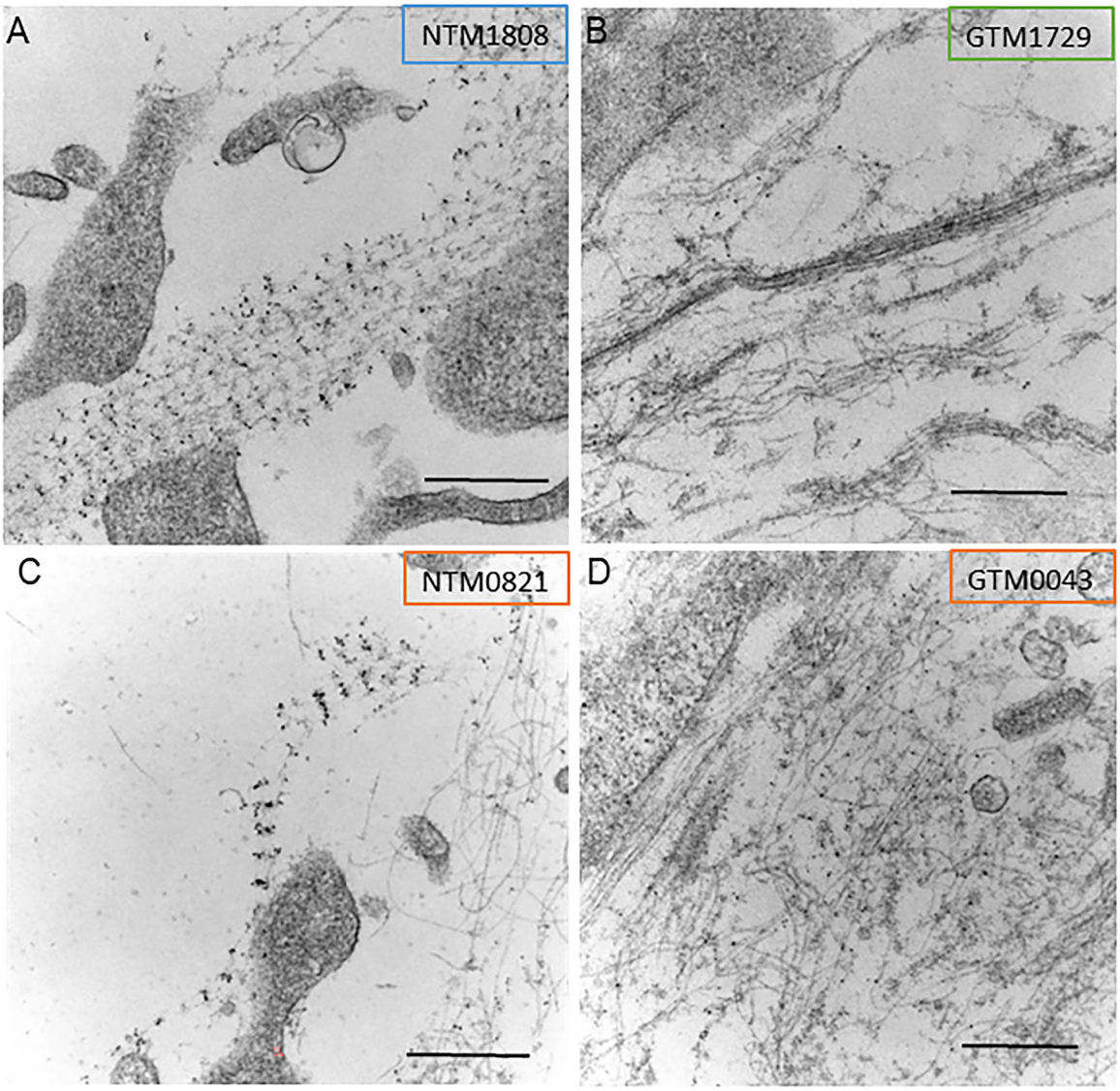

Figure 4. Transmission electron microscopy of human TM cell strains in culture.

Immuno-gold identification of type VI microfilaments using a COL6A3 monoclonal antibody of (A) NTM1808, (B) GTM1729 and two cell strains harboring the TSP1 N700S gene variant, (C) NTM0821 and (D) GTM0043. Scale bar = 500 nm.

Table 1.

Clinical findings in family members classified as POAG, ocular hypertensive (grey) and glaucoma suspect (darker grey).

Pedigree #	Age*	Gender	IOP+ OD/OS	C/D OD/OS	Optic Nerve~ OD/OS	Visual field loss OD/OS	CCT OD/OS	Surgery
IV20	77	M	29/35	0.4/0.45	Glaucomatous/ Suspicious	unreliable/ unreliable	ND	OS
IV3	73	M	24/33	0.45/0.8	Glaucomatous/ Suspicious	Glaucomatous/ glaucomatous	548/555	
IV7	55	M	27/44	0.9/1	Glaucomatous OU	ND	600/ND	
V7	48	M	25/25	0.2/0.5	Suspicious / glaucomatous	Unreliable/ normal	ND	
IV9	60	F	25/23	0.9/0.9	Suspicious / glaucomatous	Suspicious/ glaucomatous	547/560	OU
IV11	73	M	13/25	0.9/0.9	Glaucomatous OU	ND	ND	
IV37	73	F	23/24	0.4/0.5	Normal/ glaucomatous	Suspicious / glaucomatous	574/593	
V37	54	M	33/28	0.8/0.8	Glaucomatous OU	Suspicious / glaucomatous	555/558	
IV13	67	F	28/28	0.7/0.7	Glaucomatous OU	Normal OU	ND	
V11	76	F	30/28	0.9/0.9	Glaucomatous OU	Unreliable OU	587/589	
IV16	77	M	24/27	0.6/0.8	Suspicious / glaucomatous	Normal/ glaucomatous	512/512	
IV18	70	F	32/36	0.9/0.9	Suspicious OU	Normal/normal	559/553	OU
IV23	67	F	20/36	0.7/0.7	Glaucomatous OU	Glaucomatous/ glaucomatous	ND	OS
IV25	64	F	20/23	0.8/0.8	Glaucomatous OU	Glaucomatous/ glaucomatous	526/509	OU
IV5	38	M	21/22	0.8/0.8	Glaucomatous OU	Glaucomatous/ glaucomatous	509/510	
IV26	79	F	21/22	0.7/0.6	Glaucomatous OU	Glaucomatous/ glaucomatous	505/506	
V23	51	F	21/18	0.6/0.6	Glaucomatous /Normal	Suspicious /normal	575/585	
IV10	75	M	20/17	0.7/0.1	Glaucomatous /Normal	Glaucoma/ normal	560/549	
V33	58	M	19/18	0.9/0.8	Glaucomatous OU	Glaucomatous/ glaucomatous	506/504	OS
V1	56	M	28/28	0.7/0.65	Glaucomatous/ Suspicious	Normal OU	461/493	
IV4	78	M	19/23	0.1/0.3	Normal OU	Normal OU	549/547	
V4	56	M	24/24	0.4/0.4	Normal OU	Normal OU	628/611	
V36	76	F	23/29	0.7/0.6	Suspicious OU	Suspicious OU	ND	
IV19	64	F	27/27	0.3/0.3	Normal OU	Normal OU	ND	
V8	64	F	24/23	0.4/0.4	Normal OU	ND	567/566	
VI5	53	F	28/28	0.3/0.2	Normal OU	Normal OU	539/538	
IV38	78	F	18/19	0.5/0.4	Suspicious OU	Normal OU	577/580	
V35	73	M	18/18	0.7/0.8	Suspicious OU	Suspicious OU	534/553	

Pedigree #	Age*	Gender	IOP+ OD/OS	C/D OD/OS	Optic Nerve~ OD/OS	Visual field loss OD/OS	CCT OD/OS	Surgery
V39	69	F	14/14	0.5/0.5	Glaucomatous/ suspicious	Normal/ Suspicious	601/606	
VI8	57	M	18/18	0.5/0.6	Glaucomatous OU	Normal OU	558/552	
VI1	63	M	13/13	0.1/0.3	Normal/ suspicious	Normal OU	528/522	
V18	54	M	18/18	0.5/0.5	Suspicious OU	Suspicious /normal	547/561	

*Age at diagnosis for POAG patients.

+highest known IOP.

~as determined by a clinician.

ND – not done.

Table 2.

Association of Extracellular Matrix SNPs with POAG in Large Pedigree.

SNP	Location*	Gene Symbol	Gene Name	Function	Minor Allele Frequency^
rs2228262	15:39882178	*THBS1*	Thrombospondin-1	N700S	10.6%
rs112913396	2:238289767	*COL6A3*	Collagen, type VI, alpha 3	D563G	0.1%
rs62638750	19:10084460	*COL5A3*	Collagen, type V, alpha 3	V1195A	0.8%
rs34759087	3:49162284	*LAMB2*	Laminin subunit beta 2	E987K	11.3%
rs11545200	11:65319751	*LTBP3*	Latent transforming growth factor beta binding protein-3	A438V	7%
rs11690358	2:238244781	*COL6A3*	Collagen, type VI, alpha 3	M2988V	11.2%
rs11586699	1:183184690	*LAMC2*	Laminin subunit gamma 2	T124M	9.6%

^1000 Genomes European Population

*From GRCh37.p13 Assembly

Table 3:

χ2-tests by Clinical Variable.

		POAG		Hypertension		Heart attack	
SNP	**Gene**	**p-value**	**adjusted p-value***	**p-value**	**adjusted p-value***	**p-value**	**adjusted p-value***
rs2228262	*THBS1*	0.004	0.031	>.999	>.999	0.034	0.103
rs62638750	*COL5A3*	0.083	0.417	0.343	>.999	0.602	>.999
rs112913396	*COL6A3*	0.005	0.031	0.057	0.115	0.121	0.121
rs34759087	*LAMB2*	0.789	>.999	0.235	0.940	0.676	>.999
rs11545200	*LTBP3*	0.648	>.999	0.281	0.844	0.209	0.836
rs11690358	*COL6A3*	0.548	>.999	>.999	>.999	>.999	>.999
rs11586699	*LAMAC2*	0.598	>.999	0.279	0.894	>.999	>.999

*Adjusted by the Holm's method

Table 4.

Demographics and Genotyping of Normal and Glaucomatous Human TM Cell Strains.

HTM cell strain	Age	Sex	Cause of Death	*TSP1* rs2228262	*COL6A3* rs112913396	*LAMB2* rs34759087	Glaucoma Status
2011–0644	22	M	massive head trauma	A_A	A_A	C_C	-
2011–1808	19	M	multiple trauma	A_A	A_A	C_C	-
2012–0821	43	F	anoxic brain injury	A_G	A_A	C_C	-
2012–0885	3	M	probable abdominal sepsis, possible bacterial meningitis	A_A	A_A	C_T	-
2012–1457	47	M	ventricular fibrillation arrest	A_G	A_A	C_C	-
2012–1507	46	M	repatorenal syndrome	A_A	A_A	C_C	-
2012–1587	23	M	cardiac arrest	A_A	A_A	C_T	-
2016–1304	20	M	multiple blunt force trauma	A_A	A_A	C_C	-
2017–1379	33	F	drug overdose	A_A	A_A	C_C	-
2017–1472	41	M	cardiac arrest	A_A	A_A	C_C	-
2017–1480	34	M	alcoholic liver disease	A_A	A_A	C_C	-
2018–0070	54	M	cardiac arrest; end stage renal disease	A_A	A_A	C_C	-
2018–1233	53	M	lung cancer with metastases	A_A	A_A	C_C	-
2018–1341	55	M	myocardial infarction	A_A	A_A	C_T	-
2018–1783	38	M	respiratory failure	A_A	A_A	C_C	-
2019–0624	34	M	hypoxemic cardiac arrest	A_A	A_A	C_C	-
2019–1024	18	M	orbital compartment syndrome 2/2 trauma	A_A	A_A	C_T	-
2020–0982	44	M	Interstitial lung disease	A_A	A_A	C_C	-
2020–0984	69	M	Advanced Parkinson's, dementia	A_A	A_A	C_C	-
2017–1729	64	F	anoxic brain injury, cardiopulmonary arrest	A_A	A_A	C_T	Glaucoma
2018–0043	76	M	renal failure, cardiogenic shock	A_G	A_A	C_C	Glaucoma
2018–0374	79	M	ischemic cerebrovascular accident	A_G	A_A	C_C	Glaucoma OS: timolol 1 gtt q AM, IOL OS.
2018–0524	83	M	cardiac and respiratory arrest	A_A	A_A	C_C	Glaucoma (2000), IOL OU, macular degeneration
2018–1672	57	M	respiratory failure	A_A	A_A	C_C	Glaucoma (dx-2001; tx w eye drops per NOK)
2018–1898	68	M	septic shock	A_A	A_A	C_C	Glaucoma (recent dx), IOL OU
2019–0406	81	F	septic shock	A_G	A_A	C_C	Open angle glaucoma OD, IOL OU, maculopathy OU, mild NPDR OS

HTM cell strain	Age	Sex	Cause of Death	*TSP1* rs2228262	*COL6A3* rs112913396	*LAMB2* rs34759087	Glaucoma Status
2019–0461	96	F	Non ST elevation myocardial infarction	A_A	A_A	C_C	Glaucoma OU (brimonidine & latanoprost gtt OU), macular degeneration, IOL OU